

The influence of surface roughness and pre-oxidation state on the wettability of aluminium nitride by commercial brazes

N. YU. TARANETS

Institute for Materials Science Problems of the National Ukrainian Academy of Sciences, 3 Krzhyzhanovsky Str., Kiev-142, 03142 Ukraine
E-mail: taranets@ipms.kiev.ua

H. JONES*

University of Sheffield, Department of Engineering Materials, Sir Robert Hadfield Building, Mappin Str., Sheffield, S1 3JD, UK
E-mail: k.a.burton@sheffield.ac.uk

The effects of roughness ($R_a = 0.17\text{--}0.20\ \mu\text{m}$) and of pre-oxidation of the AlN ceramic surface on its wettability and contact interaction with commercial brazing alloys CB4 and CB5 of Ag-Cu-Ti composition have been studied. Wettability has been determined by the sessile drop method at three holding temperatures (810, 900 and 950°C). Particularities of the interface interaction have been identified by microprobe analysis for pre-oxidized samples. Experimental data are compared with data for samples polished to $R_a = 0.02\text{--}0.03\ \mu\text{m}$ not subjected to pre-oxidation. The results show that, for the systems under study, surface roughness does not influence the contact angle value significantly. Pre-oxidation of the AlN in air at 1250°C, however, tends to reduce wettability as a result of the replacement of braze-aluminium nitride interaction by braze-surface aluminium oxide interaction. © 2004 Kluwer Academic Publishers

1. Introduction

Pre-oxidation and roughness are two typical surface conditions that apply to non-oxide ceramics involved in industrial manufacturing processes. The problem is that, during production, the oxidation state is difficult to prevent and polishing is difficult to perform except for ceramic parts of very simple shape. The influence of these variables on the contact angle and interaction for high temperature solid/wetting alloy systems, such as ceramic/Ti-containing alloy systems, has not been studied very much experimentally.

A study [1], performed for the systems quartz/Cu, Sn, Sn-Ti melts, indicated a rise in contact angle with increasing roughness for both wettability and non-wettability cases, attributed to the pinning of the triple line by surface asperities. Investigation of the Al, AlSi11/TiN systems [2] showed that the Al/TiN system is not as sensitive to roughness as the AlSi11/TiN system, because of formation of a rough interfacial layer between Al and TiN, which concealed the initial surface topography and so compensated for roughness differences between samples.

Compared with non-oxidized TiC, pre-oxidation enhanced wetting of TiC by Me-Al (Me: Au, Ag, Cu, Sn) melts [3]. This phenomenon was attributed to the reduction of the oxidized layer by Al and subsequent transfer

of the released Ti into the molten alloy. According to [4], contact angles of Sn and Ni on oxidized α -SiC are governed up to 1600 K by the presence of a SiO₂ film on the surface. The actual interface Me/SiC is developed only when fragmentation of the SiO₂ takes place at temperatures above 1600 K. The Me/SiC interface thus develops in course of time during such isothermal exposure, as for the system Cu-Si alloys/oxidized SiC [5]. This is because silicon in the alloy provides *in situ* cleaning of the substrate surface by reaction with the oxide layer, resulting in the formation of volatile SiO.

Only one work is known to the authors which reports on contact angles of Ag-Cu-Ti alloys in contact with a pre-oxidized ceramic [6]. Melts of two compositions (1.5 and 2 wt%Ti) in contact with oxidized SiC ceramics were studied. As in [4], the silica surface film retarded the action of Ti in promoting wettability and so pre-oxidation of SiC lead to an increase in contact angles.

As shown by the above, the effects of roughness and pre-oxidation are difficult to predict from general considerations and need to be investigated for each particular system.

Aluminium nitride based ceramic is a modern material for electronics and other applications where its high thermal conductivity and high electrical resistivity

* Author to whom all correspondence should be addressed.

play an important role. Its particular areas of application make its brazability an important requirement.

The goal of the present work was to determine the extent to which pre-oxidation and roughness of an AlN ceramic affect its wettability and interaction with commercial Ag-Cu-Ti brazes that have not been studied previously and so assess the degree to which the surface variables need to be controlled during its preparation for brazing. Results obtained for oxidized AlN and for AlN polished to average roughness $R_a = 0.17\text{--}0.20\ \mu\text{m}$ are compared with related results reported elsewhere [7] for AlN polished to $R_a = 0.02\text{--}0.03\ \mu\text{m}$ not subjected to pre-oxidation in contact with the same brazes under the same experimental conditions.

2. Experimental procedure

The sessile drop method was used for the contact angle measurements. The high temperature vacuum furnace employed for the experiments has been described elsewhere [6]. The main part of the furnace is a horizontal mullite tube heated externally by a nichrome wire heating element. The optical system of the apparatus produced an image of the drop with magnification of up to ~ 1.5 times on a photo film. The magnification of the resulting image on the photographic prints used for measurements, was about 10 times.

Fully dense AlN samples made by liquid phase sintering were supplied by the Saint Gobain Ceramic Company. During firing, YAM (YAlO_3) additive (up to 3–5 wt%) was used as a sintering aid. The dimensions of samples used for the experiments were about $15 \times 15 \times 2\ \text{mm}$. Two brazing alloys, CB4(70.5Ag-26.5Cu-3Ti: wt%) and CB5(64Ag-34.2Cu-1.8Ti: wt%) were supplied by the BrazeTec GmbH Company. Alloys were supplied in the form of wire 3 mm in diameter. The wire was cut before the experiments into cylinders of height about 3 mm and mass about 0.2 g.

Experiments were performed at 810, 900 and 950°C under a vacuum better than $1 \times 10^{-3}\ \text{Pa}$. The lowest temperature, 810°C, was chosen as the highest point of the melting range of the more refractory brazing alloy. Temperature was raised at 3°K/min up to 810°C and at 4°K/min above 810°C. The time when the furnace reached 810, 900, 950°C was designated as the zero time point for contact angle measurements, although the beginning of melting was observed at temperatures of about 780°C, which is the lowest point of the brazes' melting interval.

Contact angle and base diameter of the drop were measured versus time of isothermal exposure at the indicated temperatures. The contact angle was accounted as final if it did not change by more than 1–2° during a further isothermal exposure of 20 min and the base diameter of the drop did not increase measurably during the same time interval.

Ceramic substrates for experiments were ground and polished to $R_a = 0.17\text{--}0.20\ \mu\text{m}$ by finishing with a water-based 3 μm diamond suspension. This will be described as the rougher surface compared with $R_a = 0.02\text{--}0.03\ \mu\text{m}$ obtained in Ref. [7] by finishing polishing with a 1 μm diamond suspension. These samples

were annealed in vacuum at 800°C for 20 min. Pre-oxidation was performed in air at 1250°C for 30 min on samples previously polished to $R_a = 0.02\text{--}0.03\ \mu\text{m}$. Prior to the experiments, all samples were ultrasonically cleaned in acetone and alcohol.

Some of the sessile drop samples were subsequently cross-sectioned vertically and prepared metallographically for investigation by scanning electron microscopy (SEM). A JeoL JXA-880R microprobe (at the University of Oxford) and Jeol 6400 were used for the SEM work.

3. Results

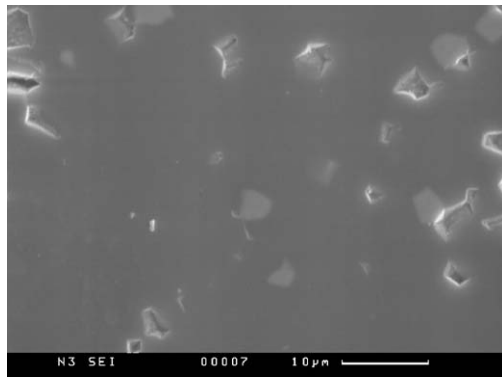
Results on wettability experiments for rougher polished ($R_a = 0.17\text{--}0.20\ \mu\text{m}$) and pre-oxidized samples are presented in comparison with results for finer polished samples ($R_a = 0.02\text{--}0.03\ \mu\text{m}$) reported earlier [7].

Secondary Electron Images (SEIs) of the surface of samples of the two levels of roughness presented in Fig. 1a and b show that their relief differs significantly. Contact angle versus time data for rougher samples are compared with finer polished samples from [7] in Fig. 2a and b, which show that the systems under study are not very sensitive to the two roughness levels and the final contact angles and the times to reach them are very similar for the two levels of roughness.

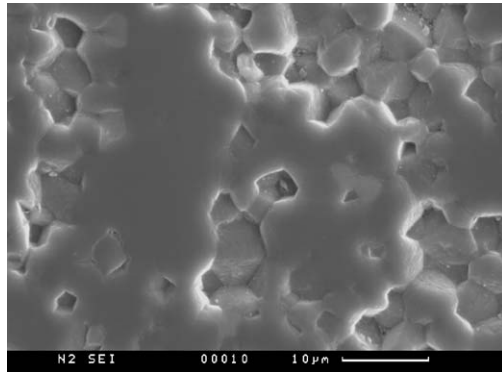
Comparison of SEI images for samples with and without pre-oxidation treatment (Fig. 1a and c) shows the presence of a continuous oxide film in Fig. 1c. X-ray Diffraction (XRD) analysis of the pre-oxidized substrate shows that this film is basically Al_2O_3 (Fig. 3). Time-temperature dependencies of contact angle (Fig. 4a and b) for surfaces with and without pre-oxidation show as a whole worse wettability after pre-oxidation in that contact angles are increased. However, the presence of the oxide film does not influence the time of spreading, i.e., the final contact angle has been reached in the same time for pre-oxidized as for non-oxidized samples.

Microstructure of the cross-sections for pre-oxidized samples (Fig. 5a and b) shows a zone of new products at the interface for both CB4 and CB5. The zone consists of two continuous layers 1 and 2 and is thicker for CB4 melt with the higher Ti content. A considerable number of inclusions are evident in the solidified melt near the reaction zone for the CB4 sample. An oxide film present on the surface of the ceramic cannot be seen on Back-Scattered Electron Images (BEIs), but it can be distinguished on corresponding oxygen X-ray maps (Fig. 5c presents one for a CB4 sample). The general distribution of metallic elements is similar for both melts and is presented for CB4 in Fig. 5d and e. It shows a significant concentration of Ti in the interaction zone.

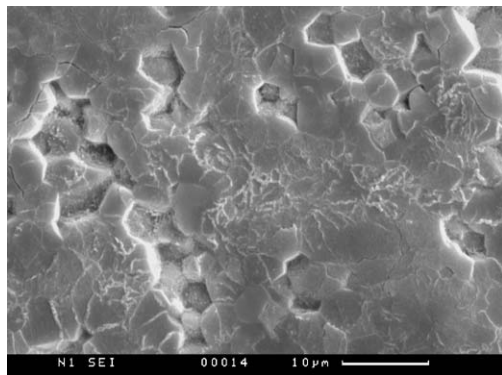
Microprobe data (at.%) for pre-oxidized samples are presented in Table I. They are similar for CB4 and CB5 melts. Analysed points from the layer of ceramic surface oxide film (Fig. 5c) gave compositions of two stoichiometric atomic ratios: (1) Al/O = 1/1.5 with 0 or 1.4 at.% Ti at these points and (2) Al/O = 1/2.5–4.6 with 11 to 32 at.% Ti. The stoichiometric ratio obtained for



(a)



(b)



(c)

Figure 1 SEIs of the surface of AlN ceramic: (a) polished to $R_a = 0.02\text{--}0.03\ \mu\text{m}$, (b) polished to $R_a = 0.17\text{--}0.20\ \mu\text{m}$ and (c) pre-oxidized.

layer 1 is $\text{Ti}_1/\text{O}_{0.5\text{--}0.6}/\text{Cu}_{0\text{--}0.15}/\text{Ag}_{0\text{--}0.02}$. The composition of layer 2 is $\text{Ti}_1/\text{O}_{0.4\text{--}0.5}/\text{Cu}_{1\text{--}1.2}/\text{Ag}_{0.01\text{--}0.1}$. Inclusions in CB4 alloy near the layer 2 are of composition $\text{Ti}_1/\text{Cu}_{0.7\text{--}1.1}/\text{Ag}_{0.6\text{--}0.9}/\text{O}_{0.3\text{--}0.4}$. Similar inclusions in CB5 alloy have composition $\text{Cu}/\text{Ag}_{0.6}/\text{Ti}_{0.4}/\text{O}_{0.2}$. Small quantities of nitrogen and yttrium were detected for some points in the interaction zone and adjacent metallic phase and Al was detected for all analysed points.

4. Discussion

4.1. Effect of surface roughness

The main factors affecting wettability on a rougher surface compared to a polished one are discussed in detail elsewhere [8–11]. They can be defined as follows:

(1) The solid-liquid interfacial contact area is larger for the wetted rougher sample than for the smoother

one. This means that, for the same base drop diameter, a higher actual surface area will be covered by the liquid if the surface is rougher. For a system with a positive wetting tendency this provides a larger energy driving force to induce spreading and so a rougher surface should be wetted better. This can be expressed as:

$$\cos \theta = r \cos \theta_0 \quad (1)$$

where θ_0 is the contact angle on a smooth surface; θ is the contact angle on the rough surface and r is the ratio of the real surface area to that of its planar projection.

(2) Advancing contact angle on a rough surface should be higher than on a polished surface by the average inclination of rough asperities to the plane surface. So the visible contact angle is the sum of two values: the equilibrium contact angle and that of the asperities slope, i.e., the rougher surface is wetted less effectively, as represented by:

$$\theta = \theta_0 + \alpha \quad (2)$$

where α is the average inclination of asperities to the plane surface.

(3) Contact angles generally do not reach the value predicted by (1) or (2) due to the fact that rough asperities create a series of energy barriers to the advancing liquid, which can be overcome or not depending on the size of the barrier and the vibration energy of the liquid. Like (2), this results in a higher contact angle for a rougher surface. Experimentally, such an increase in apparent contact angle with increase in substrate roughness has been reported for high temperature ceramic-metal systems for both wettability and non-wettability cases as follows: Ni-Cr, Ni-Y/ Al_2O_3 [12]; Ga, Sn, Ni/ SiO_2 , Cu/HfC [11]; Al, AlSi11/TiN [2].

This contrasts with the results of the present study, in which no significant difference was observed for the final contact angles of CB4 and CB5 melts between $R_a = 0.17\text{--}0.20\ \mu\text{m}$ and $R_a = 0.02\text{--}0.03\ \mu\text{m}$ AlN. That does not necessarily mean that the factors mentioned above are not applicable to the systems and conditions under study, but it seems that any effect they had was too small to be detected.

A non-wettability case for which the difference in contact angles between the two levels of roughness tends to zero is reported in [9] and was associated with formation of a “composite interface,” comprising solid-liquid and solid-vapour sections. It is formed when liquid cannot infiltrate surface valleys and contacts the surface only at hill tops so there is no pinning effect of slopes. This mechanism cannot be applied to the systems under study however, because the liquid phase wets the ceramic well and, moreover, reacts with its surface.

Evidently, the reaction, the initial ceramic surface involved, and the particularities of the drop spreading for the melts under study result in similar wettability for the two levels of roughness studied. In Ref. [7] it was concluded for CB4 and CB5 on AlN that a thin Ti-rich

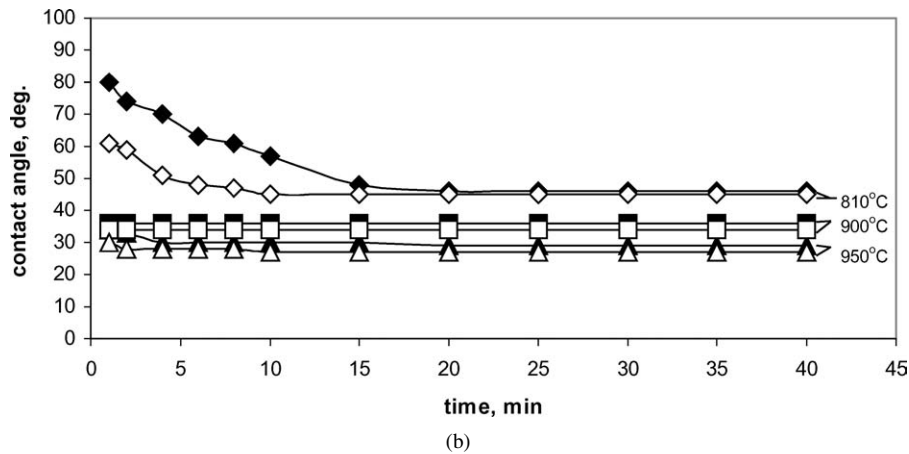
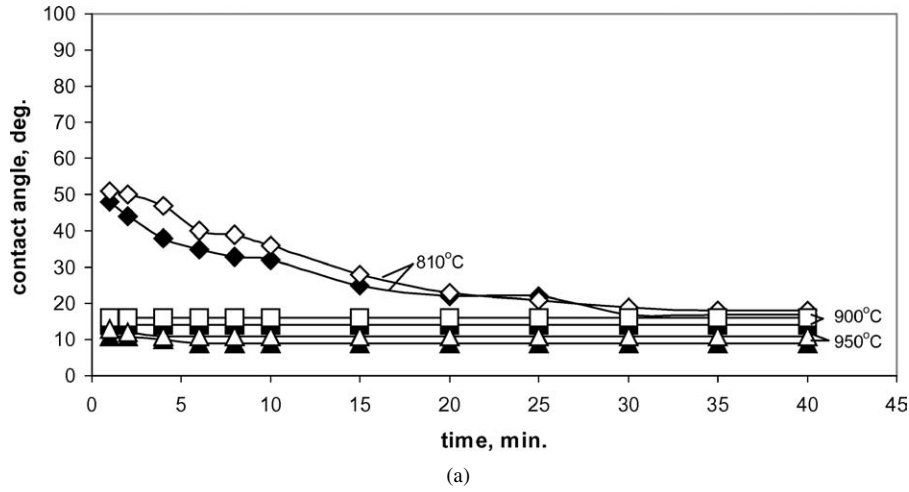


Figure 2 Time and temperature dependencies of contact angles for: (a) CB4 and (b) CB5 melts on AlN ceramic of roughness $R_a = 0.17\text{--}0.20 \mu\text{m}$ (open points) in comparison with data from Ref. [7] for samples polished to $R_a = 0.02\text{--}0.03 \mu\text{m}$ (closed points).

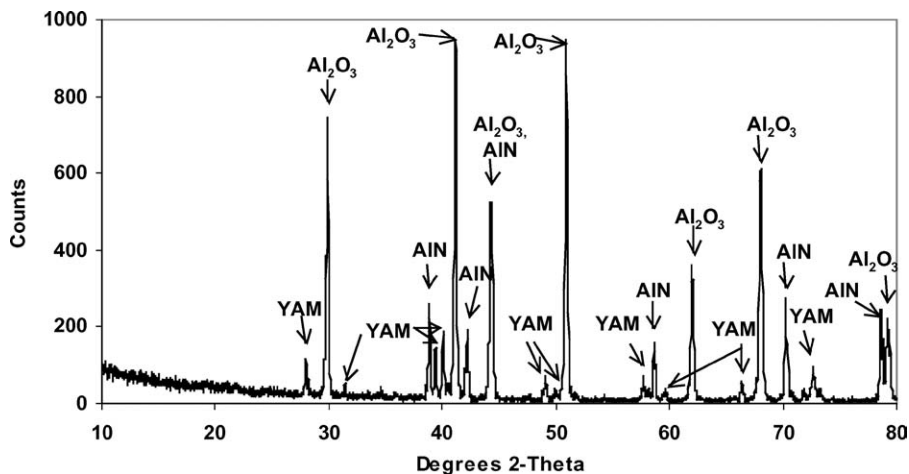


Figure 3 XRD-pattern from the surface of the pre-oxidized AlN ceramic.

film of melt spreads ahead of the mass of the melt and modifies the surface. Bulk metal then moves over the preliminary film forming a visible contact angle. The operation of this mechanism on a rougher surface could account for the absence of a difference in contact angles.

Fig. 6a–c show SEI and Ti X-ray images of an AlN surface revealed as a result of CB5 shrinkage after a sessile drop experiment at 810°C without any extended isothermal exposure. Fig. 6a–c indicate that a continuous layer of products containing Ti covers the exposed surface. Clearly, due to the high chemical affinity of

titanium to nitrogen, the melt reacts with and modifies the surface while spreading. So, the thin film, advancing ahead of the bulk melt, modifies the surface, destroying hills and valleys. Macro contact angle depends on the roughness of the new surface relief. The relief for cases under study is not defined by the extent of previous polishing, but by the roughness of the created interface products. Roughness of the created interface was also considered have influenced the final contact angle for the systems Al, AlSi11/TiN [2] and Al/C [13].

TABLE I Results (at.%) of microprobe analysis of interaction layers for the pre-oxidized ceramic with CB4 and CB5 corresponding to Fig. 5a and b

Braze and layer	N	Ti	Cu	Ag	Al	O	Y	No of analysed points
CB4								
Oxide film	1.5	0	0.16	0.25	38	60	0.02	1
Oxide film	0.71, 0.76	13, 14	0.4, 1.3	0.5, 0.9	23.2 ± 0.1	60.8 ± 0.1	0.03 ± 0.05	2
Layer 1	0.08 max	62.1 ± 1.5	8.1 max	0.21 ± 0.06	0.8 max	35.3 ± 3.1	0.01 max	4
Layer 2	0	38.2 ± 0.3	39.8 ± 0.3	0.20 ± 0.03	4.6 ± 0.1	17.2 ± 0.7	0	3
Alloy	0.14 max	34 max	70 max	30 max	2.1 ± 0.3	9.7 ± 1.9	0.01 max	4
CB5								
Oxide film	1.5	0, 1.4	0.17	0.07, 0.19	37, 40	58	0.004, 0.007	2
Oxide film	0.4, 1.1	11, 31	0.2, 0.3	0.4	12, 25	55, 62	0.012	2
Layer 1	0.3 max	58.8 ± 7.2	9.3 max	1.2 max	5.3 max	35.6 ± 4.0	5.5 max	5
Layer 2	0	36.6 ± 0.9	42.9 ± 2.6	2.9 max	1.4 ± 0.1	17.7 ± 0.8	0.004 ± 0.001	3
Alloy	0	0 or 17	81 max	89 max	0.18 ± 0.07	7.9 max	0	4

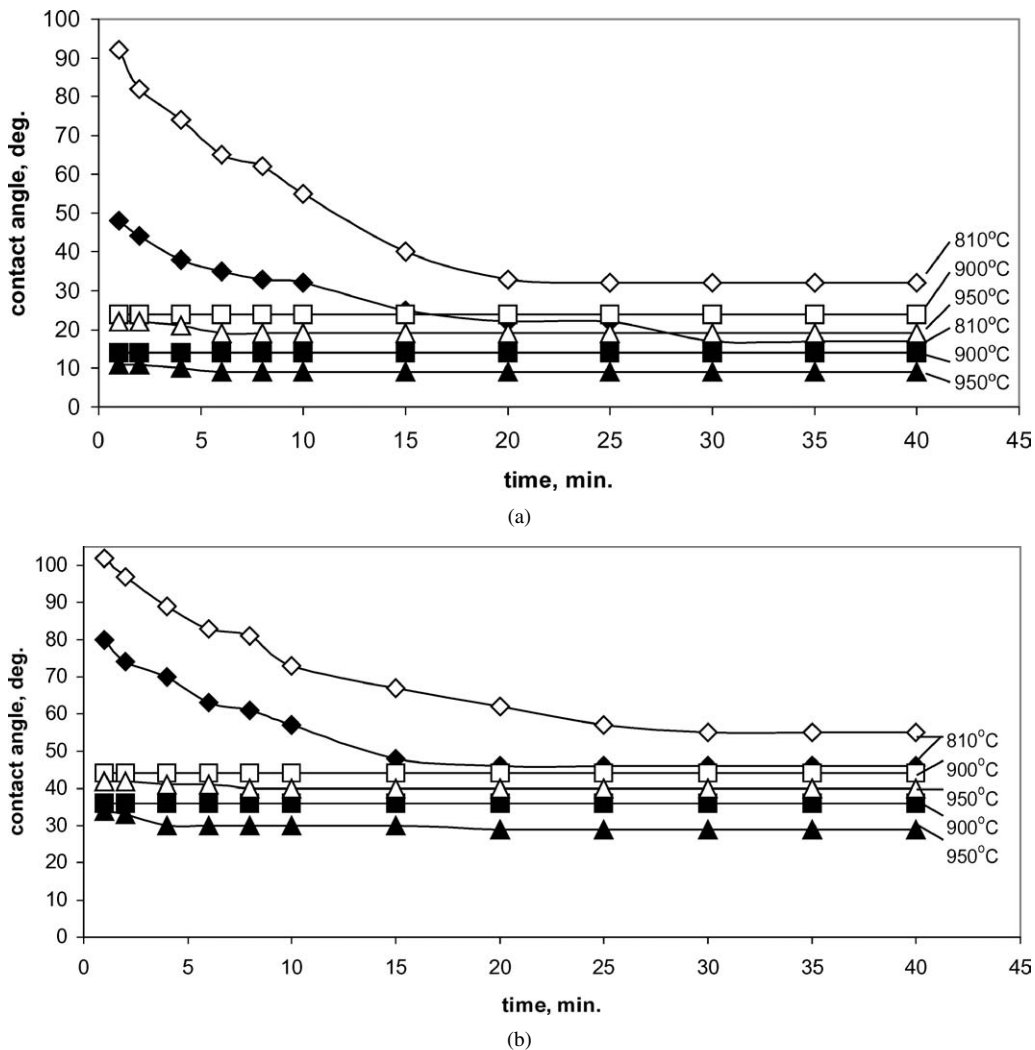
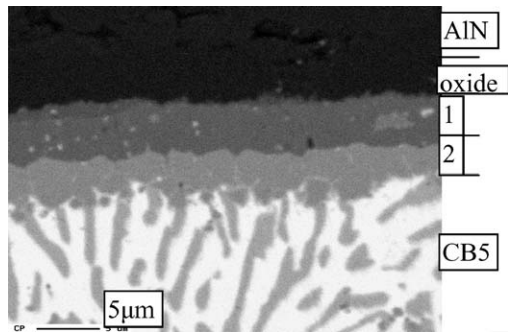


Figure 4 Time and temperature dependencies of contact angles for: (a) CB4 and (b) CB5 melts on the pre-oxidized AlN (open points) in comparison with results from [7] for polished ($R_a = 0.02\text{--}0.03\ \mu\text{m}$) non-preoxidized samples (closed points).

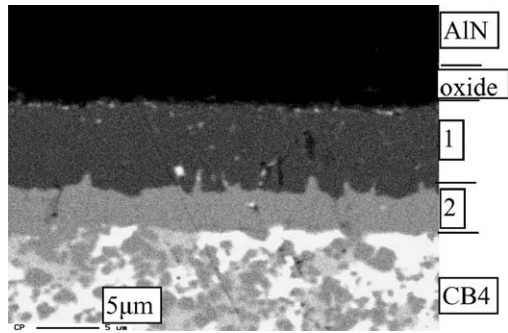
4.2. Effect of pre-oxidation

The present results on contact angles reveal that pre-oxidation of the AlN tends to reduce wettability compared to non-preoxidized samples (Fig. 4). The same was observed in [6] for Ag-Cu-Ti alloys in contact with pre-oxidized SiC ceramic and in [4] for Sn and Ni on oxidized SiC. This difference, evidently, results from different mechanisms of interface interaction for non- and preoxidized samples.

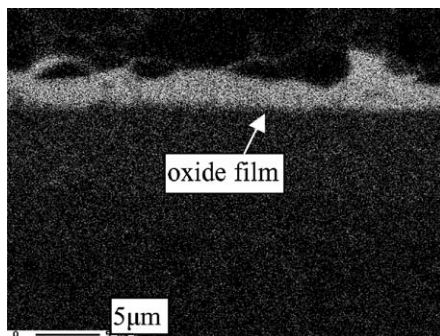
The XRD-pattern for the pre-oxidized AlN surface (Fig. 3) shows that aluminium oxide in the form of Al_2O_3 is present on the surface of the material. The SEI image of the surface shows that the film covering the surface has a network of cracks in it (Fig. 1c). It was also established elsewhere [14] that oxidation of AlN in air at temperatures above 1100°C produces a layer of Al_2O_3 on the surface, and that thermal stresses due to differences in thermal expansion coefficients between



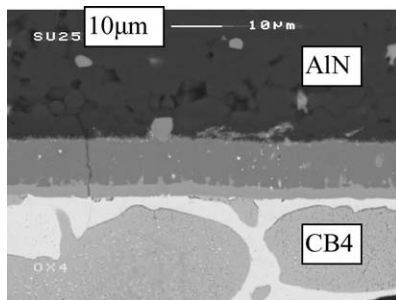
(a)



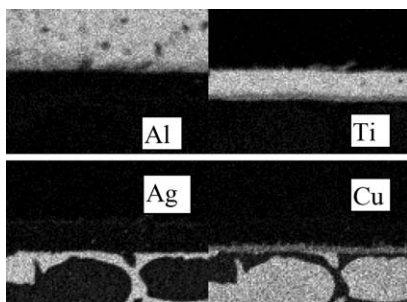
(b)



(c)

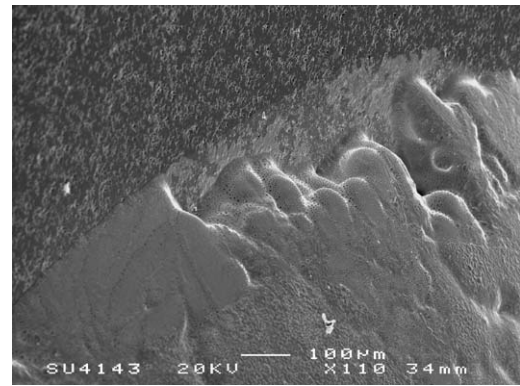


(d)

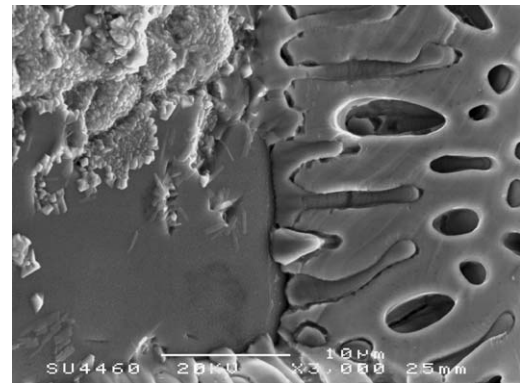


(e)

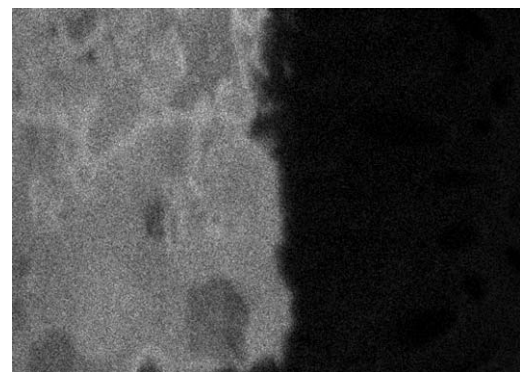
Figure 5 SEM images of the interface microstructure for pre-oxidized AlN in contact with CB5 and CB4 melts (temperature-time regime: 810°C-40 min, 900°C-40 min, 950°C-40 min): (a) CB5, (b) CB4 with (c) corresponding oxygen X-ray map, (d) CB4 with (e) corresponding Al, Ti, Ag and Cu X-ray maps.



(a)



(b)



(c)

Figure 6 Top views of the reacted ceramic surface ($R_a = 0.17\text{--}0.20\ \mu\text{m}$) revealed after melt shrinkage resulting from solidification after heating to 810°C and immediately cooling (a), (b) with (c) Ti X-ray map corresponding to (b).

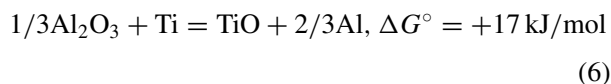
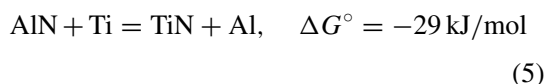
the oxide layer and the nitride generate cracks and micropores in the oxide scale.

Results for metal distributions (Fig. 5e) are similar to those for the non-preoxidized ceramic [7]. Titanium is concentrated in the interaction zone. Microprobe analysis, however, indicates that the compositions of reaction layers and products of interaction differ significantly. Table I shows that, for both brazes, nitrogen was not registered in interaction layers in quantities higher than 0.3 at.%. Registered atomic ratio of elements indicates that layer 1 (Fig. 5a and b) is composed of non-stoichiometric titanium oxide $\text{TiO}_{0.5\text{--}0.6}$. A similar compound was registered near the ceramic in the interaction layer between Al_2O_3 and 72Ag-28Cu + 1 or 5 wt%Ti formed at 1000°C [15], between Al_2O_3 and Cu-xTi (x_{Ti} up to 0.125) alloy at 1100°C [16]

and for Al_2O_3 and $58\text{Ag}39\text{Cu}2.8\text{Ti}$ at 950°C [17]. It has been also found by Transmission Electron Microscopy (TEM) [18] for an alumina/Ag40Cu57Ti3 couple (1000°C), that the reaction product near the alumina consists of TiO. The presence of detectable quantities of Ag and Cu in layer 1 in the present study can be identified with their inclusions between TiO grains. Inclusions may result from non-active metal components being trapped in the process of TiO grain formation.

Layer 2's compositions are different from layer 1's and for both melts can be written as $\text{Ti}_1\text{Cu}_{1-1.2}\text{O}_{0.4-0.5}$, which corresponds to a compound of type $\text{Cu}_2\text{Ti}_2\text{O}$. A similar ratio was previously registered in ref. [16] for the part of the interaction zone further from the alumina. The quantities of Al registered in the liquid phase and reaction zone exceed the permitted maximum content of Al in CB4 and CB5 brazes (0.001% according to the BrazeTec GmbH Technical Datasheet), this Al must have been released from decomposition of Al_2O_3 during interaction. It should be also noted that according to the Ti, Al and O quantities in Table I and Fig. 5c, part of the alumina layer remains on the AlN surface and contains inclusions of non-stoichiometric TiO.

The main reaction product observed in the present study (non-stoichiometric TiO) differs significantly from the main product (non-stoichiometric TiN) registered after interaction of non-preoxidized AlN with CB4 and CB5 [7]. Moreover, no TiN was registered as an interaction product with the pre-oxidized AlN and, instead, reaction products correspond to those observed previously for $\text{Al}_2\text{O}_3/\text{Ag-Cu-Ti}$ couples. The following conclusions can be drawn: the reaction products in the interaction layers of AlN/CB4,5 couples after pre-oxidation of AlN in the regime under study are replaced by reaction products of $\text{Al}_2\text{O}_3/\text{CB4,5}$ couples. That takes place in spite of the fact that formation of Al_2O_3 is not a thermodynamically preferred reaction at temperatures around 900°C :



where the data for ΔG° for calculations are taken from [19]. The thermodynamic analysis as to why the reaction (6) does proceed at the $\text{Al}_2\text{O}_3/\text{AgCuTi}$ boundary is discussed in detail elsewhere [16].

As to the present findings, it is evident that the oxide film on the surface of the ceramic inhibits the reaction between Ti and AlN and results instead in the reaction of Ti with Al_2O_3 . This is accompanied by an increase in thermodynamic stability of the solid phase ($\Delta G_{900^\circ\text{C}}^\circ(\text{AlN}) = -224 \text{ kJ/g-at.N}$, $\Delta G_{900^\circ\text{C}}^\circ(\text{Al}_2\text{O}_3) = -465 \text{ kJ/g-at.O}$ [19]). Generally, at least for the same kind of substances, poorer wettability is observed with a rise in the thermodynamic stability of the solid phase [20]. Evidently, that is the basis for the higher contact angle values observed for the pre-oxidized samples.

5. Conclusions

1. Prior polishing of the AlN surface to $R_a = 0.17-0.20 \mu\text{m}$ compared with $R_a = 0.02-0.03 \mu\text{m}$ has no significant effect on its contact angle with CB4 or CB5 brazing alloys, or on the time to reach the final contact angle at 810 to 950°C .

2. Pre-oxidation of the AlN surface increases both initial and final contact angles with CB4 and CB5 brazing alloys but does not affect significantly the time to reach the final contact angle at 810 to 950°C .

3. Interaction of pre-oxidized AlN with CB4 and CB5 gives layered interaction zones that increase in width for the increased Ti content of CB4, and lie adjacent to the residue of the original alumina film generated by pre-oxidation.

4. These findings are explained on the basis that interaction between the braze metal and AlN obliterates any differences in roughness between the two levels investigated, so no difference in contact angle or time to reach the final contact angle results, while the reduced wettability resulting from pre-oxidation is a consequence of interaction taking place with an alumina film rather than with the underlying aluminium nitride.

Acknowledgements

The authors are grateful to The Royal Society of UK for visitorships to enable N. Yu. Taranets to carry out this research at the University of Sheffield (Project refs. No AMM/UA/13402/01A and 15458).

References

1. YU. V. NAIDICH and V. S. ZHURAVLEV, in "Poverhnostrnie yavleniya v rasplavah i obrazuyuschihsiya iz nih tverdyh fazah" (Kabardino-Balkarskoe Knizhnoe Izdatel'stvo, Nal'chik, 1965) p. 245 (in Russian).
2. N. SOBCZAK, K. PIETRZAK, A. WOJCIECHOWSKI, W. RADZIWIŁŁ, M. KSIAZEK and L. STOBIEŃSKI, *Trans. JWRI*. **30** (2001) 173.
3. N. FROUMIN, N. FRAGE and M. DARIELL, in Proc. 10th Internat. Ceramic Congress. Part C, edited by P. Vincenzini (Techna, Faenza, 2003) p. 733.
4. A. TSOGA, S. LADAS and P. NIKOLOPOULOS, *Acta Mater.* **45** (1997) 3515.
5. O. DEZELLUS, F. HODAJ, C. RADO, J. N. BARBIER and N. EUSTATHOPOULOS, *ibid.* **50** (2002) 979.
6. J. LOPEZ-CUEVAS, H. JONES and H. V. ATKINSON, *Mater. Sci. Eng. A* **266** (1999) 161.
7. N. YU. TARANETS and H. JONES, *Mater. Sci. Eng. A*, in press.
8. R. SHUTTLEWORTH and G. L. J. BAILEY, *Discuss. Faraday Soc.* **3** (1948) 16.
9. R. E. JOHNSON and R. H. DETTRE, *Advan. Chem.* **43** (1964) 112.
10. J. D. EICK, R. J. GOOD and A. W. NEUMANN, *J. Coll. Interf. Sci.* **53** (1975) 235.
11. S. J. HITCHCOCK, N. T. CARROLL and M. G. NICHOLAS, *J. Mater. Sci.* **16** (1981) 714.
12. R. M. CRISPIN and M. NICHOLAS, *ibid.* **11** (1976) 17.
13. K. LANDRY, S. KALOGEROPOULOU and N. EUSTATHOPOULOS, *Mater. Sci. Eng. A* **254** (1998) 99.
14. D. SURYANARAYANA, L. MATIENZO and D. SPENCER, *IEEE Trans. Comp. Hybrids Manuf. Technol.* **12** (1989) 566.

15. R. E. LOEHMAN and A. P. TOMSIA, *Acta Metall. Mater.* **40** (Suppl.) (1992) S75.
16. P. KRITSALIS, L. COUDURIER and N. EUSTATHOPOULOS, *J. Mater. Sci.* **26** (1991) 3400.
17. W. BYUN and H. KIM, *Scripta Metall. Mater.* **31** (1994) 1543.
18. D. JANICKOVIC, P. SEBO, P. DUHAJ and P. SVEC, *Mater. Sci. Eng. A* **304–306** (2001) 569.
19. D. R. STULL and H. PROPHET, "JANAF Thermochemical Tables," 2nd ed. (NSRDS-NBS 37, 1971).
20. Y. NAIDICH, in "Progress in Surface and Membrane Science," Vol. 14, edited by D. A. Cadenhead and J. F. Danielly (Academic Press, New York, 1981) p. 354.

*Received 4 August 2003
and accepted 29 April 2004*